n-type InP substrates [8]. This influence of the LD structure on the resistance is thought to be conspicuous in ZnSe-based LDs, because the electron mobility of ZnSe is much smaller than that of InP. Actually, the differential resistance at the current density of 500A/cm² is ~18Ω for the homo-epitaxial ZnSe-based LDs and is two times larger in magnitude than that of the ordinary ZnSe-based LD structure grown on n-type GaAs substrates. The increase in the differential resistance for the homo-epitaxial LDs is mainly attributed to the additional sheet and contact resistance of the n-type ZnSe contact layer. Therefore it is believed that the use of highly conductive n-type ZnSe substrates would be effective at both reducing the diode resistance and suppressing the temperature rise in the active layer for homo-epitaxial LDs.

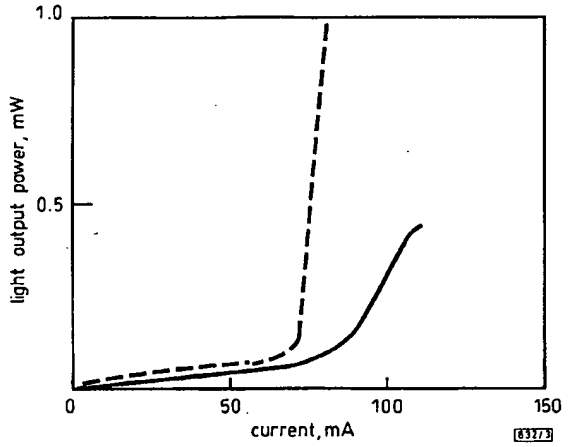

Fig. 3 *Light output-current characteristics of homo-epitaxial LD at room temperature*

——— CW operation
– – – – pulsed operation
T = 298K

In conclusion, we have achieved room temperature CW operation of ZnSe-based blue-green laser diodes, homo-epitaxially grown for the first time on semi-insulating ZnSe substrates. The threshold current and the operation voltage under CW operation were 84mA and 15V, respectively. The differential resistance of homo-epitaxial LDs was two times larger than that of hetero-epitaxial LDs grown on n-GaAs. It is important that highly conductive n-type ZnSe substrates become commercially available to improve the characteristics of homo-epitaxial LDs.

Acknowledgment: The authors would like to thank Y. Matsuoka and H. Iwamura for their encouragement in this work.

2 April 1997
Electronics Letters Online No: 19970624

A. Ohki, T. Ohno and T. Matsuoka (*NTT Opto-electronics Laboratories, 3-1, Morinosato Wakamiya, Atsugi-shi, Kanagawa Pref., 243-01, Japan*)

Y. Ichimura (*Hewlett-Packard Laboratories Japan, 3-2-2, Sakado, Takatsu-Ku, Kawasaki-Shi, Kanagawa Pref., 213, Japan*)

References

1 HAASE, M.A., QIU, J., DEPUYDT, J.M., and CHENG, H.: 'Blue-green laser diodes', *Appl. Phys. Lett.*, 1991, **59**, (11), pp. 1272–1274

2 TANIGUCHI, S., HINO, T., ITOH, S., NAKANO, K., NAKAYAMA, N., ISHIBASHI, A., and IKEDA, M.: '100h II-VI blue-green laser diode', *Electron. Lett.*, 1996, **32**, (6), pp. 552–553

3 NAKANO, K., and ISHIBASHI, A.: 'Characterization of ZnMgSSe-based wide-gap laser diodes'. Extended abstracts Int. Conf. Solid State Devices and Materials, 1996, pp. 62–64

4 GUHA, S., DEPUYDT, J.M., HAASE, M.A., QIU, J., and CHENG, H.: 'Degradation of II-VI based blue-green light emitters', *Appl. Phys. Lett.*, 1993, **63**, (23), pp. 3107–3109

5 NAKATSUKA, S., GOTOH, J., MOMOSE, M., TAIKE, A., and KAWATA, M.: 'Crystal defect behavior and analytical modeling of life-time in II-VI blue-green optoelectric devices'. Proc. Int. Symp. Blue Laser and Light Emitting Diodes, Chiba, 1996, pp. 232–235

6 OHNO, T., OHKI, A., and MATSUOKA, T.: 'Investigation of degradation in homoepitaxially grown ZnCdSe/ZnSe light emitting diode', to be published in *Jpn. J. Appl. Phys. Lett.*, 1997, **36**, pp. 190–193

7 SCHETZINA, J.F.: 'Homoepitaxy of widegap II-VI and III-V Compounds'. Proc. Int. Symp. Blue Laser and Light Emitting Diodes, Chiba, 1996, pp. 74–79

8 MATSUOKA, T., TAKAHEI, K., NOGUCHI, Y., and NAGAI, H.: '1.5μm region InP/GaInAsP buried heterostructure lasers on semi-insulating substrates', *Electron. Lett.*, 1981, **17**, (1), pp. 12–14

Improvement of f_T by dipole doping at the collector heterojunction in InP double HBTs

S.P. McAlister, W.R. McKinnon and R. Driad

Indexing terms: Semiconductor heterojunctions, Heterojunction bipolar transistors, Semiconductor doping

The authors show clearly how dipole doping at the collector heterojunction in an InP/InGaAs double heterojunction bipolar transistor improves device performance. Specifically, both f_T and f_{MAX} are increased and the DC current-blocking is reduced. Also the DC switching characteristics, seen in devices with abrupt undoped InGaAs/InP collector heterojunctions, can almost be eliminated by using the dipole doping at that interface.

Introduction: The composite-collector design for double HBTs [1] improves the breakdown performance of the devices, and the design of the collector heterojunction and collector doping profile can help improve the high frequency performance, without compromising the DC characteristics. In this Letter we compare devices whose only difference is the doping near the collector heterojunction, showing clearly the improvement of both the RF and the DC performances. The energy barrier at the InGaAs/InP heterojunction in the collector can degrade the DC performance at high current densities, and can also cause a switching behaviour [2, 3]. The collector barrier blocks electron flow when it extends above the base conduction band, for the case of ballistic electrons and also when the electrons are thermalised [4]. This blocking effect causes a buildup of stored charge in the collector and limits the high-speed performance, as measured by f_T for example.

A complicated competition between tunnelling and thermionic emission of electrons across the heterojunction in the collector produces the DC switching effects seen in some composite-collector DHBTs [3]. In general, the switching is related to the existence of S- or N-shaped negative differential conductivity (NDC) and leads to hysteresis in a voltage-controlled experiment [3]. Experimentally, the effect is best seen in the device's common-base characteristics, although the common-emitter characteristics also displays the effect.

In composite-collector HBTs there are various approaches to reducing the effects of the energy barrier at the InGaAs/InP interface by modifying the electric field distribution, for example through δ-doping [5] or grading of the junction [6]. Here we show clearly how dipole-doping [7] at the InGaAs/InP interface improves f_T, as well as the DC characteristics.

Epitaxial structure and devices: Table 1 shows the details of the epitaxial layer structures, grown by gas-source MBE by Tutcore Ltd., that were used for the devices. The lattice-matched alloy $In_{0.53}Ga_{0.47}As$ is referred to as InGaAs. The collector structure incorporates a spacer layer of InGaAs between the base and the InP in the collector. Dipole-doping [7] can increase the electric field over a thin layer and narrow the energy barrier at a heterojunction. The two layer designs differ only in the doping at the InGaAs/InP heterojunction in the collector. In the wafer, referred to as 'dipole-doped', extra doping was added near the InGaAs/InP interface. The top 10nm of InP before the InGaAs/InP interface was n-doped to $10^{18}cm^{-3}$ (this gives an areal density of $10^{12}cm^{-2}$), and the first 10nm of InGaAs after the interface was p-doped to the same level. The dipole-doping at the InGaAs/InP interface narrows the barrier so that electrons should be able to tunnel through the top part of it.

Table 1: Epitaxial layer structure

Material	Thickness	Doping	Density
	μm		cm^{-3}
InGaAs	0.10	*n* (Si)	2×10^{19}
InP	0.06	*n* (Si)	2×10^{19}
InP	0.09	*n* (Si)	3×10^{17}
InGaAs	0.01	undoped	—
InGaAs	0.05	*p* (Be)	2×10^{19}
InGaAs	0.05	*n* (Si)	5×10^{15}
InP	0.30	*n* (Si) or dipole-doped	5×10^{15}
InP	0.008	*n* (Si)	5×10^{18}
InGaAs	0.45	*n* (Si)	5×10^{18}
InP	substrate	SI (Fe)	—

Large-area devices were fabricated with wet chemical etching and had a triple mesa structure, as did the high frequency ones. The latter devices differed in having self-aligned emitters, and had high frequency pads on conformal SiO_2 to contact the device through via holes in the oxide. The large-area devices ranged in emitter area from $50 \times 50\mu m^2$ to $70 \times 90\mu m^2$,whereas the high frequency devices were as small as $3 \times 5\mu m^2$.

Results and discussion: Gummel plots for large-area devices with identical emitter areas, made from the two different epitaxial structures, gave almost identical characteristics, confirming that the emitter and base structures are essentially the same and that the device fabrication was reproducible. The DC gain at V_{BE} = 0.5V was ~90, and the base and collector currents did not cross down to $< 10^{-11}$ A . For both layer designs the breakdown voltages at room temperature exceeded 8V.

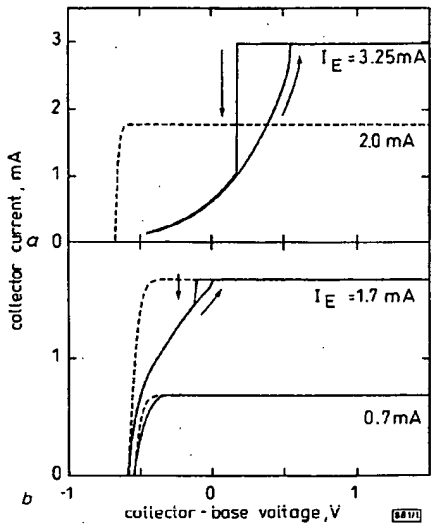

Fig. 1 *Common-base characteristics*

a At 100K for undoped collector device compared with dipole-doped transistor
b At 295K for $6 \times 10\mu m^2$ high frequency devices
——— undoped collector device
– – – – dipole-doped device
Devices had $70 \times 90\mu m^2$ emitter areas

In Fig. 1*a* the common-base characteristics at 100K for the undoped collector structure (solid lines in the Figure) show the switching behaviour: at low V_{CB} the collector current I_C is significantly smaller than its ultimate value of $\alpha_0 I_E$. This is due to the blocking effect of the collector heterojunction [4]. If V_{CB} is ramped down to 0V from an initial value of 1.5V the curves show the hysteresis, which is the result of the underlying *S*-shaped nature of the I-V characteristic. With the incorporation of dipole-doping at the collector heterojunction there is no evidence (dashed line in Fig. 1*a*, also at 100K) of the current-blocking, switching or hysteresis as seen for the previous device. The devices in Fig. 1*a* are large-area devices ($70 \times 90\mu m^2$ emitter area) where the current densities are low. In Fig. 1*b* the room temperature common-base characteristic for a $6 \times 10\mu m^2$ high frequency device, with the undoped collector structure, still displays the switching and current-blocking effect. For increasing I_E, the voltage of which I_C attains the limiting value $\alpha_0 I_E$ shifts to higher voltages. This is important to remember when performing experiments against I_E. The dashed line in Fig. 1*b* shows the corresponding results for a dipole-doped device at room temperature.

The high-speed performance can be compromised when composite-collector HBTs show switching or current-blocking because of the collector heterojunction. As a result of the current blocking, a large concentration of electrons builds up in the potential well formed at the barrier in the collector [4]. This extra stored charge will increase the charging time of the device and so reduce its high frequency performance. Fig. 2 compares the variation of f_T and f_{MAX} for devices with and without the dipole-doped collector structure. The results for the undoped collector device do not extend beyond 20mA due to the current-blocking, which complicates experiments. At a fixed V_{CE}, where, at low currents, the biasing conditions put the device above the region where there is current-blocking, eventually at higher currents this is not so, and the experiments cannot be properly carried out. This is because the blocking/switching regime moves to higher voltages as I_E increases. (This point is illustrated in the case of the common-base characteristics by reference to the data in Fig. 1*b*. For example, at V_{CB} = 0.5V and with low currents, the device looks normal, but eventually at a high enough value of I_E, the current blocking region occurs for this voltage. Any experiment that looks at a dependence on I_C or I_E is eventually effected.)

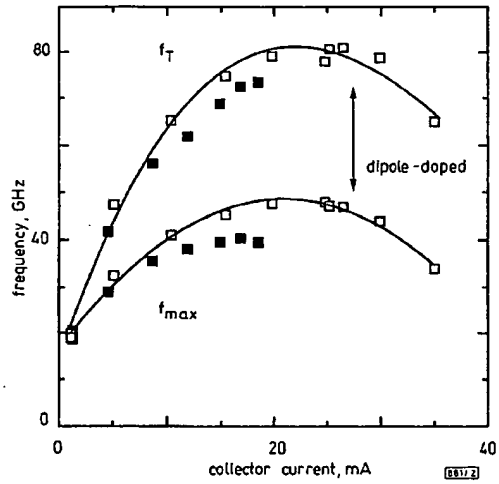

Fig. 2 *Collector current dependence of f_T and f_{MAX} for undoped and dipole-doped devices*

Devices had emitter areas of $6 \times 10\mu m^2$ and V_{CE} = 2V
■ undoped
□ dipole-doped

Devices with dipole-doping perform well, achieving a maximum value for f_T of ~80GHz (at a collector current density of $\sim 4 \times 10^4$ Acm^{-1}) for a $6 \times 10\mu m^2$ device, even though the fabrication and layer design is not aggressive. The maximum value of f_T for the dipole-doped device corresponds to a minimum total delay time of 1.97ps. We estimate the emitter charging time as ~0.43ps by extrapolating $1/(2\pi f_T)$ against $1/I_C$ to zero $1/I_C$. Note that for the dipole-doped case, the values of f_T at a given collector current are above the corresponding values for the undoped collector device, showing that dipole-doping reduces the stored charge in the collector. As Fig. 1 shows, there is no evidence of current-blocking effects in dipole-doped devices with emitter areas of $50\mu m^2$. It must be checked whether the blocking is also eliminated for devices with still smaller emitters. If it is not eliminated, there is room to narrow the barrier still further, by replacing the uniform doping in our design by δ-doped layers on either side of the barrier.

Conclusions: We have demonstrated how dipole-doping at the collector heterojunction in composite-collector DHBTs leads to a

better high frequency performance, as a result of a reduction in the current-blocking and switching behaviour found in designs which do not incorporate the dipole-doping.

Acknowledgments: We would like to thank A. Renaud, S. Laframboise and D. Scansen for help in performing the measurements.

7 April 1997

Electronics Letters Online No: 19970644

S.P. McAlister, W.R. McKinnon and R. Driad (*Device Physics, Institute of Microstructural Sciences, National Research Council of Canada, Ottawa, K1A 0R9, Canada*)

References

1 FEYGENSON, A., RITTER, D., HAMM, R.A., SMITH, P.R., MONTGOMERY, R.K., YADVISH, R.D., TEMKIN, H., and PANISH, M.B.: 'InGaAs/InP composite collector heterostructure bipolar transistors', *Electron. Lett.*, 1992, **28**, pp. 607

2 RITTER, D., HAMM, R.A., FEYGENSON, A., TEMKIN, H., and PANISH, M.: 'Bistable hot electron transport in InP/GaInAs composite collector heterojunction bipolar transistors', *Appl. Phys. Lett.*, 1992, **61**, pp. 70

3 MCALISTER, S.P., MCKINNON, W.R., ABID, Z., and GUZZO, E.E.: 'Hysteresis in the switching of hot electrons in InP/InGaAs double-heterojunction bipolar transistors', *J. Appl. Phys.*, 1994, **76**, pp. 2559

4 MCKINNON, W.R.: 'One-flux analysis of current blocking in double-heterostructure bipolar transistors with composite collectors', *J. Appl. Phys.*, 1996, **79**, pp. 2762

5 TOKUMITSU, E., DENTAI, A.G., JOYNER, C.H., and CHANDRASEKHAR, S.: 'InP/InGaAs double heterojunction bipolar transistors grown by metalorganic vapor phase epitaxy with sulphur delta doping in the collector region', *Appl. Phys. Lett.*, 1990, **57**, pp. 2841

6 KURISHIMA, K., NAKAJIMA, H., KOBAYASHI, T., MATSOKA, Y., ISHIBASHI, T., and : 'Fabrication and characterization of high-performance double-heterojunction bipolar transistors', *IEEE Trans. Electron Devices*, 1994, **41**, pp. 1319

7 CAPASSO, F., CHO, A.Y., MOHAMMED, K., and FOY, P.W.: 'Doping interface dipoles: Tunable heterojunction barrier heights and band-edge discontinuities by molecular beam epitaxy', *Appl. Phys. Lett.*, 1985, **46**, pp. 664

ESTIMATION OF LENGTH FOR *ELECTRONICS LETTERS* VERSION 5.0

Title	0.5 column cm per 40 characters (or part thereof)		
Indexing terms	1.5 column centimetres (this includes adjacent space)		
Abstract	1 column cm per 165 characters		
Text	1 column cm per 165 characters (it is easiest to estimate the number of characters, including spaces, per line and the number of lines per page)		
References	1 column cm each		
Tables	0.4 column cm per line		
Figures	All figures are reduced to fit within an 8.6 cm × 8.6 cm box. If the figure is wider than it is high, divide the height by the width and multiply by 8.6 column cm. If the figure is higher than it is wide (discouraged), the figure will occupy 8.6 column cm.		
Captions	1 column cm per main figure or table caption (provided it is brief), 0.33 column cm per line for subcaptions (including keys and other information that will be removed from the figures).		
Equations	Single line equations:	0.6–0.8	column cm per line
	Integrals:	1.0	column cm per line
	Quotients:	0.7–1.2	column cm per line
	Sums and products:	1.2	column cm per line
	Matrices:	0.4	column cm per line
	For other equation types, refer to a recent issue of *Electronics Letters*. Excessively long equations will be split into several lines.		